The calibration method of the circle-structured light measurement system for inner surfaces considering systematic errors

OPEN ACCESS
IOP Publishing
Measurement Science and Technology
Meas. Sci. Technol. **32** (2021) 075012 (12pp)
https://doi.org/10.1088/1361-6501/abe288

The calibration method of the circle-structured light measurement system for inner surfaces considering systematic errors

Yuchu Dong, Changshuai Fang, Linlin Zhu, Ning Yan and Xiaodong Zhang

State Key Laboratory of Precision Measuring Technology & Instruments, Laboratory of Micro/Nano Manufacturing Technology, Tianjin University, Tianjin 300072, People's Republic of China

E-mail: zhangxd@tju.edu.cn

Received 17 November 2020, revised 25 January 2021
Accepted for publication 2 February 2021
Published 6 May 2021

Abstract

Light plane deviation and motion direction deviation of stage systems are the two main sources of systematic errors in circle-structured light inner surface measurement systems. In this paper, we propose a new two-step calibration method to compensate these systematic errors. In the first step, a more accurate initial light plane calibration result is obtained by multi-position binocular-structured light calibration. Then, in the second step, the initial result is optimized by measuring the inner radius of a standard ring gauge to obtain the optimal light plane calibration result. Based on this result, the real motion direction is also calibrated by optimization using the inner surface scanning measurement data of the standard ring gauge. The proposed method improves the system calibration accuracy through the second calibration step, making it convenient to operate without using complex calibration targets or expensive equipment. Therefore, this calibration method has the potential to be used in actual measurements. The experimental results show that the mean relative measurement error can reach 0.015% in our homemade measurement system and validate that the measurement system calibrated by our proposed method realizes high-precision and high-repeatability measurements for inner surfaces.

Keywords: circle-structured light measurement, inner surface measurement, system calibration

(Some figures may appear in colour only in the online journal)

1. Introduction

With the progress of manufacturing technology, many parts with special inner surface structures are manufactured and used in energy engineering, chemical industry, aerospace and other fields [1]. The inner surfaces are designed to contain grooves, freeform surfaces, holes or other structures to meet their usage requirements, and their machining quality directly affects work performance [2–4]. Therefore, it is important to find a reliable and accurate three-dimensional (3D) inner surface measurement method for quality inspection [5, 6]. To realize inner surface measurement, researchers have proposed several methods, such as contact measurement [7], the laser ranger finder [8], multi-color digital holographic inspection [9, 10], white light interferometry [11] and circle-structured light measurement [12, 13]. Among them, circle-structured

light measurement is a special kind of structured light measurement method that uses laser triangulation. Compared to common point- or line-structured light measurement methods [14, 15], it can directly form a 360° projection light stripe on an inner surface and measure the whole inner surface with high efficiency and without complicated operations or using a complex system structure [16]. However, the measurement accuracy of the circle-structured light system is mainly affected by two sources of systematic error: light plane deviation and motion direction deviation of the stage system. Therefore, these systematic errors need to be calibrated and compensated for to ensure measurement accuracy.

The light plane deviation caused by assembly errors in the structured light generator mainly leads to low measurement accuracy, so there are many reports on circle-structured light calibration methods to compensate for this systematic error. These methods can be divided into three categories. Firstly, the calibration method based on vision measurement principle by Wang *et al* [17] used a concentric circle coplanar reference object to calibrate the circle-structured light plane based on the cross-ratio invariance. This method requires a high-precision stage to move the reference object along the axis of the circle-structured light. Zhu *et al* [18, 19] proposed the binocular-structured light calibration method. The camera in the system and another auxiliary camera form a binocular system to obtain the coordinates of light stripes formed by a blank planar board intersecting the structured light to fit the light plane parameters. This method has a low demand on instruments and is easy to operate. However, in [19], the binocular observation range of the structured light plane during calibration is limited by the system structure, leading to a relatively low measurement repeatability. Secondly, the calibration method using calibration targets from Zhuang *et al* [20] calibrates the system by measuring a standard ring gauge and comparing the result with its reference radius. This method requires strict parallel between the main axis of the measurement system and the axis of the ring gauge, which is difficult to implement. Buschinelli *et al* [21, 22] calibrated their system to measure an inner stepped cylindrical gauge with 28 different diameter regions to obtain a polynomial relation between the pixel radius of ring light stripes and the real radius. The inner surface is calculated according to this relation. This method relies on a high-precision calibration target with a complex structure and its operation is intricate. Thirdly, a method utilizing other measurement equipment by Zhang *et al* [23, 24] used two electric theodolites to measure the coordinates of light spots formed by intersecting a thin thread with structured light to fit the light plane. This method has relatively high calibration accuracy but requires expensive instruments. Existing methods have defects such as complicated calibration operations, reliance on special equipment and relatively low calibration accuracy, making these methods difficult to use in industrial applications while maintaining measurement precision. Thus, it is necessary to find a low-cost and convenient structured light calibration method for high-precision measurements.

A circle-structured light system usually needs to be driven by a linear stage to scan the inner surface. In most studies, reconstructing the scanned and measured inner surface is under the default assumption that the motion direction of the stage is parallel to the main axis of the measurement system. Therefore, the systematic error in the deviation between two directions is ignored, which affects measurement accuracy. Fang *et al* [25] found that systematic errors in the motion shaft system of the structured light scanning measurement system cause the adjacent scanning data to appear as spatial displacement. However, the calibration method for this systematic error has not been well studied yet in for circle-structured light measurement systems, and this problem needs to be solved to ensure the scanning measurement accuracy.

In this paper, we researched high-precision inner surface measurement using a circle-structured light system and a circle-structured light system was built to meet the actual measurement applications. To realize high-precision measurements, we propose a new two-step system calibration method for the circle-structured light system to compensate for the systematic errors from the two sources mentioned above. In the first step, multi-position binocular-structured light calibration is conducted to obtain a more accurate initial calibration result based on a larger observation range of the light plane. Then, in the second step, the system measures the standard ring gauge to further improve the system calibration accuracy. The initial light plane calibration result is optimized using the radius measurement results of the ring gauge placed at different random positions and orientations to obtain the optimal calibration result. Using this result, the motion direction is calibrated by optimization using the inner surface scanning measurement data of the ring gauge to compensate for the systematic errors in reconstructing the scanned surface. In this new method, the optimization process using the standard ring gauge measurement data in the second step can reduce the influence of the binocular measurement error on structured light calibration in the first step to ensure system calibration accuracy. Meanwhile, this method can be implemented easily without using complex calibration targets or expensive equipment. Therefore, the proposed calibration method can help measurement systems achieve high-precision measurements in industrial applications. The experiments were carried out on our homemade measurement system, and the results demonstrate that the new calibration method can ensure system measurement accuracy in real measurement applications.

2. Model of the measurement system

A model of the circle-structured light measurement system is shown in figure 1, O_c-$x_cy_cz_c$ is the camera coordinate system, which is taken as the measurement coordinate system. z_c is the main axis of the system and the axis of the structured light generator is aligned with it. The beam emitted by the laser is reflected by the conical reflector to generate circle-structured light, and it intersects with the inner surface to form a ring light stripe that is captured by the camera. The light stripe image is processed by the upper system to obtain the surface measurement result by the laser triangulation algorithm. The whole system is mounted on a linear stage.

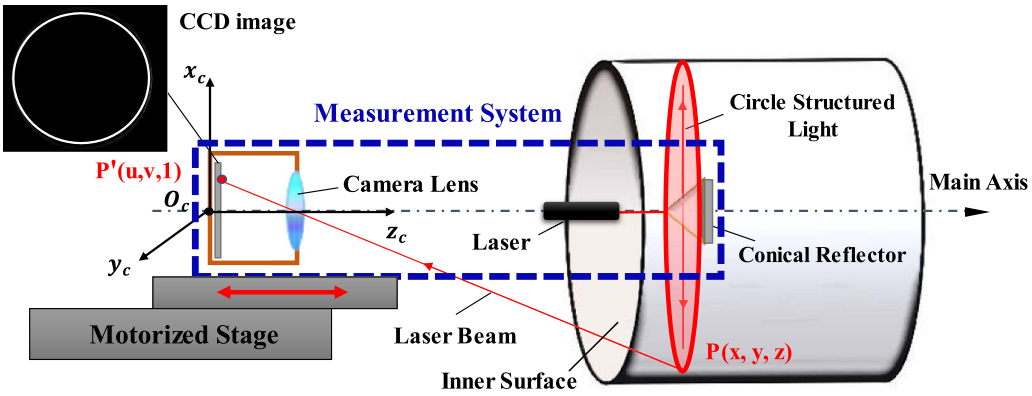

Figure 1. Construction model of the circle-structured light inner surface measurement system.

As shown in figure 1, P is a point on the position where the structured light intersects the inner surface. In the system model, the camera uses a pinhole model to describe the projection relationship between object points and image points. It is assumed that the coordinates of P are $(x,y,z)^T$ in the camera coordinate system, and that the homogeneous coordinates of the image point P' is $(u,v,1)^T$. The relationship between P and P' can be expressed as follows:

$$\rho P' = AP \tag{1}$$

$$A = \begin{bmatrix} f_x & \alpha & u_0 \\ 0 & f_y & v_0 \\ 0 & 0 & 1 \end{bmatrix}. \tag{2}$$

In equation (1), ρ is a scale coefficient and A is the intrinsic matrix of the camera. The matrix elements are shown in equation (2). f_x and f_y are the principal distances of the camera in X-axis and Y-axis directions, and (u_0, v_0) are the coordinates of the principal point. α is the camera skew parameter. The equation of the circle-structured light plane in the camera coordinate system can be expressed as follows:

$$\begin{cases} Ax + By + Cz + D = 0 \\ A^2 + B^2 + C^2 = 1. \end{cases} \tag{3}$$

In equation (3), $(A\ B\ C\ D)$ are parameters of the structured light plane and $[A, B, C]^T$ is the unit vector of plane normal. Based on equations (1) and (3), the laser triangulation algorithm under ideal conditions can be obtained as shown in equation (4). If the parameters are determined, the coordinates of P can be obtained by solving the equation set in equation (4):

$$\begin{cases} f_x x + \alpha y + (u - u_0)z = 0 \\ f_y y + (v - v_0)z = 0 \\ Ax + By + Cz + D = 0. \end{cases} \tag{4}$$

Driven by the linear stage, the measurement system can measure the entire inner surface of the measured parts, and the 3D profile of the measured inner surface is reconstructed along the motion direction of the stage. The parameters in equation (1) are obtained through Zhang's camera calibration method [26], and the structured light parameters and the motion direction are calibrated by our proposed method, as explained in the next section.

3. The two-step system calibration method

In this paper, we assume that the measurement accuracy is mainly influenced by the light plane deviation caused by assembly errors in the structured light generator and the motion direction deviation of the linear stage. In order to improve the measurement accuracy, we propose a new two-step system calibration method to calibrate the light plane parameters and the motion direction of the stage to compensate for these systematic errors. The process of the new method is shown in figure 2. The initial light plane parameters are obtained in the first step and then optimized in the second step to improve the calibration accuracy. Based on the optimized light plane calibration result, the motion direction is also calibrated in the second step. In order to better demonstrate our calibration method, this section will introduce the structured light and the motion direction calibration process, respectively.

3.1. The circle-structured light calibration

For the structured light calibration, the initial calibration result is obtained by the multi-position binocular-structured light calibration to acquire a more accurate initial result in the first calibration step. First, the camera parameters of the system camera and the auxiliary camera are calibrated by Zhang's method [26]. During the multi-position binocular-structured light calibration, keeping the measurement system stationary, the auxiliary camera is moved to K different positions ($K \geqslant 2$). The binocular-structured light calibration is carried out at each position to avoid the interference of the system structure, to observe a larger range of the light plane and to acquire more calibration points. First, the binocular relation between the system camera and the auxiliary camera is acquired through stereo calibration at each position. A blank planar board is placed to intersect the light plane forming a line light stripe

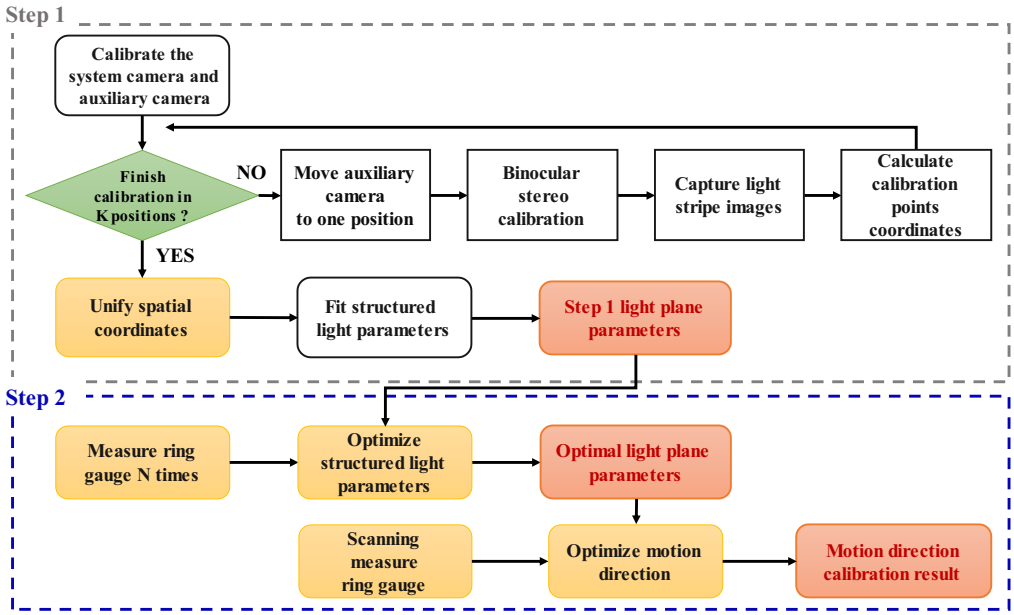

Figure 2. The flow chart of the two-step calibration method.

on it. Two cameras capture images of the light stripe simultaneously; then, the board is moved to another random position. This step is repeated M times (about 10–15 times). The central points of the light stripes are extracted as calibration points and their spatial coordinates are calculated by the binocular intersection algorithm. Then, the coordinates of the calibration points from K experiment positions are unified into the measurement coordinate system and used to fit the structured light plane parameters.

The mathematical model of the calibration experiment in one position is shown in figure 3. P represents the circle-structured light plane and B represents the planar board placed in different orientations and positions, such as B_i. O_L-$x_L y_L z_L$ and O_R-$x_R y_R z_R$ are the system camera and the auxiliary camera coordinate system. O_L-$x_L y_L z_L$ is also the measurement coordinate system. L_p and R_p are the image planes of the two cameras. z_L and z_R are the optical axes of the two cameras. O_l-$u_l v_l$ and O_r-$u_r v_r$ represent the image coordinate systems of the two cameras. The structured light plane intersects the board placed in position B_i and the light stripe L_i is formed on it. Assuming that P_{ic} is a central point on L_i, the light stripe is projected onto the image planes of the two cameras and p_{cl} and p_{cr} are the projection points of P_{ic}.

Computing the rectified images of the two cameras, O_L-$x'_L y'_L z'_L$ and O_R-$x'_R y'_R z'_R$ represent the two camera coordinate systems after epipolar rectification. It is assumed that the camera intrinsic matrix used in rectification is A, and p_{cl} and p_{cr} are transformed to p_{cl} and p'_{cr} in the rectification process. T represents the translation vector of a binocular vision system. The coordinates of P_{ic} in O_L-$x'_L y'_L z'_L$ can be calculated by equation (5):

$$P_{ic} = \frac{\|T\| A^{-1} p'_{cl}}{\|A^{-1} p'_{cl} - A^{-1} p'_{cr}\|}. \tag{5}$$

The coordinates of the calibration points are located in the respective coordinate system O_L-$x'_L y'_L z'_L$ after epipolar rectification at the K calibration positions, so the coordinates need to be unified into the measurement coordinate system O_L-$x_L y_L z_L$. Equation (6) represents the unified method. $P^k{}_{ic}$ are the coordinate of P_{ic} in the measurement coordinate system, and $R^k{}_{Lr}$ represents the epipolar rectify matrix of the system camera in the kth binocular-structured light calibration:

$$P^k_{ic} = (R^k_{Lr})^{-1} P_{ic}. \tag{6}$$

Assuming that the coordinates of $P^k{}_{ic}$ are $(x^k{}_i, y^k{}_i, z^k{}_i)^T$, the least squares method is applied to calculate the structured light plane parameters, as shown in equation (7):

$$E = \sum_{K}^{k=1} \sum_{M}^{i=1} \left(A x^k_i + B y^k_i + C z^k_i + D\right)^2. \tag{7}$$

However, this calibration result is not accurate enough to satisfy the requirements of high-precision 3D profile measurement of the circle-structured light system because the binocular measurement error will influence the calibration accuracy. Therefore, in the second calibration step, the system is used to measure the inner radius of a standard ring gauge to obtain the optimal light plane calibration result.

The inner surface of the standard ring gauge can be considered as an ideal cylindrical surface, and the intersection line of the light plane and the inner surface is an ellipse on the light plane, whose minor axis length is the inner radius measurement result [27]. However, the minor axis length of the ellipse generated by the intersection of any structured light plane and the standard ring gauge is fixed, so the ring gauge must be measured in N (N is about 10–15) different random positions and especially at different random orientations to ensure the

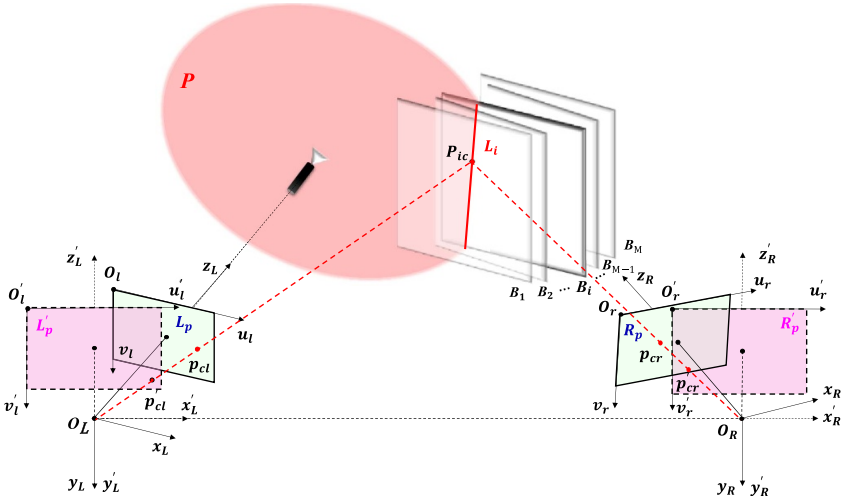

Figure 3. Mathematical model of the binocular-structured light calibration method.

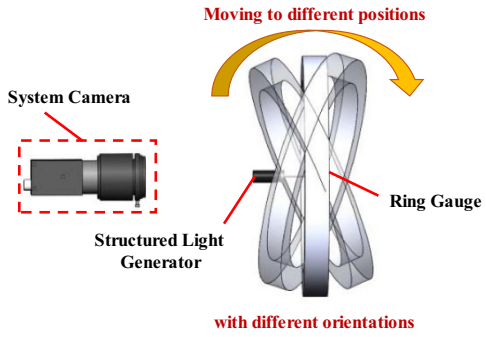

Figure 4. Moving the ring gauge to different positions with different orientations in measurement.

uniqueness and correctness of the parameter optimization result in the calibration, as shown in figure 4. At each measurement position, the system captures the image of the ring light stripe formed by the light plane intersecting the inner surface. The central points of the light stripes are extracted to obtain their pixel coordinates set p_i ($i = 1, 2, \ldots N$) in each image. The calibration result from the first step is optimized to improve the calibration accuracy using the inner radius measurement results and the reference radius R of the ring gauge using the Levenberg–Marquardt (LM) method [28]. The object function used in optimizing structured light plane parameters is represented in equation (8):

$$E = \sum_{N}^{i=1} (\text{solve}(p_i, A_L, A, B, C, D) - R)^2. \tag{8}$$

In this function, (A B C D) are parameters of the light plane parameters waiting for optimization using the pixel coordinate sets p_i and the intrinsic matrix A_L of the system camera. We used solve (p_i, A_L, A, B, C, D) to represent the process of calculating the inner radius measurement result. In this process, the spatial coordinate set P_i of the central points is calculated firstly using pixel coordinates set p_i and the intrinsic matrix A_L by laser triangulation. Then, P_i is used to fit the ellipse equation by the least squares ellipse-fitting method [29], and the inner radius measurement results R_i can be calculated by using ellipse equation parameters. The deviation between R_i and the reference radius R of the ring gauge is used as the object function to optimize the parameters (A B C D).

The structured light calibration in our method only uses an auxiliary camera, a blank planar board and a standard ring gauge without using specially designed calibration targets and expensive equipment. The calibration operation is convenient and efficient to realize high-precision calibration. There is no requirement to know the position and orientation of the board and the ring gauge exactly during the calibration process, and no need for the measurement system to maintain a specific position relationship with the ring gauge during calibration. Therefore, this method is suitable for actual measurement applications.

3.2. Stage motion direction calibration

Using the optimized structured light parameters, the real motion direction is also calibrated in the second calibration step by optimization process using the inner surface scanning measurement data of a standard ring gauge. In real measurements, the inner surface is reconstructed along this direction to ensure the scanning measurement accuracy and compensate for the systematic error.

In most studies, when reconstructing the inner surface by scanning measurement, the movement direction of the linear stage is parallel to the main axis of the measurement coordinate system. The measured surface is reconstructed by adding the measured data obtained in each step and its measurement position along the main axis direction. However, in practice, there is a deviation between the motion direction of the stage and the main axis direction caused by assembly errors between the system and the linear stage. Thus, the surface scanning measurement accuracy will inevitably decrease

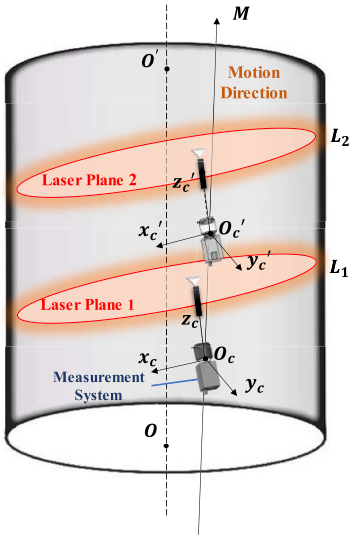

Figure 5. The model of the scanning measure process with systematic error.

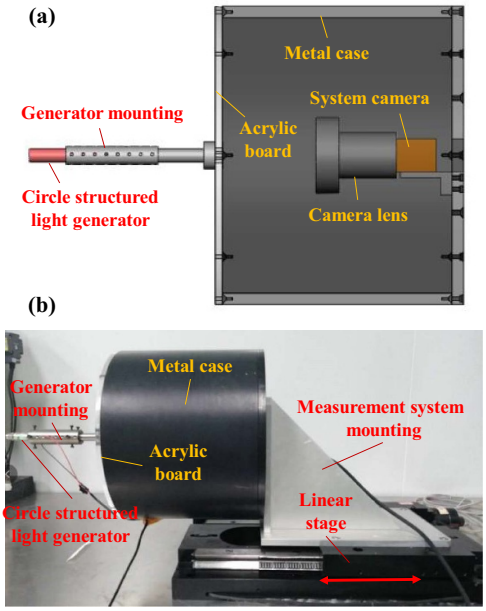

Figure 6. (a) The design diagram of the measurement system; (b) the physical map of the measurement system.

under the influence of this systematic error. A mathematical model of the inner surface scanning measurement process including this systematic error is shown in figure 5.

OO' is the axis of the measured inner surface. O_c-$x_cy_cz_c$ is the measurement coordinate system and z_c is the main axis of the measurement system. Vector **M** is the motion direction of the linear stage, and the measurement system moves along **M** which represents that the stage drives the system to scanning measure the inner surface. z_c is not parallel to vector **M** in this model representing this systematic error. In the model, the measurement system moves from position 1 to position 2 in step interval H, and measures the inner surface in two positions. L_1 and L_2 are intersecting lines of the light plane and the surface in two positions. It is assumed that the coordinates of one point on L_2 are $(x_2, y_2, z_2)^T$, and the unit vector of motion direction **M** is $[m, n, t]^T$ in the measurement coordinate system. As shown in the model, if the inner surface is to be reconstructed precisely, the motion direction should be known. The coordinates of P after reconstruction are calculated by the following equation:

$$P' = P + h\mathrm{M}. \tag{9}$$

In the second calibration step, the inner surface of the standard ring gauge is regarded as an ideal cylinder surface, and the measurement system is controlled by the stage to move forward to scanning measure the inner surface of a standard ring gauge in N steps with the step interval H. The ring gauge only needs to be scanning measured once, and can be placed at random positions and orientations during calibration. The motion direction is obtained by the LM method using the scanning measurement data and the reference radius R of the ring gauge, and equation (10) is the object function in the optimization. In this function, **M** is the motion direction that needs to be optimized, and the scanning measurement data are used to reconstruct the inner surface along the direction **M** by equation (9). n_k is the point number of the measured data set at each measurement position, and p_{ki} represents the coordinates of the measurement point. **W** represents the axis of the inner cylinder surface and S is a point on **W**. Because the spatial equation of the measured cylinder inner surface is unknown, **W** and S will also be calculated in the optimization process with the motion direction. The deviation value calculated by the object function will be used in the optimization calculation to acquire the calibrated motion direction **M**. The dot product result between the calibrated direction **M** and the positive direction of the main axis of the measurement system is >0:

$$E = \sum_{N}^{k=1} \sum_{n_k}^{i=1} \Big[(p_{ki} + (k-1)H\mathbf{M} - S)^T (\mathbf{I} - \mathbf{W}\mathbf{W}^T) \times (p_{ki} + (k-1)H\mathbf{M} - S) - R^2 \Big]^2. \tag{10}$$

In our proposed calibration method, the motion direction calibration operation is simple and it is not necessary to know the position and orientation of the ring gauge during calibration. Meanwhile, the method is highly efficient and it only takes a short time to complete the motion direction calibration. This method can be applied conveniently in actual measurements.

4. Experiment

4.1. Stage motion direction calibration

Figure 6 shows the design model and physical map. As illustrated, the light generator is composed of a 632 nm wavelength laser diode and a 90° conical reflector, which is fixed on a transparent optical grade acrylic board with 5 mm thickness through connector parts. A monochrome 10 M pixel CCD camera with a 16 mm camera lens is installed in the system as

Table 1. The simulation experiment results of structured light plane parameter optimization.

	Initial structured light plane parameters	Optimization results from the first group simulation experiment	Optimization results from the second group simulation experiment
1	[0.0440, −0.0440, 0.9980, 300.0000]	[0.0506, −0.0507, 0.9974, 301.8465]	[0.0498, −0.0499, 0.9975, 301.9996]
2	[−0.0500, 0.0500, 0.9975, 300.0000]	[0.0494, −0.0493, 0.9975, 302.0198]	[0.0499, −0.0498, 0.9976, 302.0006]
3	[−0.0500, 0.0500, 0.9975, 305.0000]	[0.0496, −0.0493, 0.9976, 301.9881]	[0.0499, −0.0499, 0.9975, 301.9997]
4	[0.1000, −0.1000, 0.9899, 305.0000]	[0.0502, −0.0503, 0.9975, 302.0108]	[0.0499, −0.0499, 0.9975, 301.9994
5	[0.0000, 0.0000, 1.0000, 295.0000]	[0.0504, −0.0506, 0.9974, 302.0137]	[0.0499, −0.0499, 0.9975, 302.0004]

Table 2. The simulation experiment results of motion direction optimization.

	Preset motion direction	Optimized motion direction	Direction deviation
Group 1	[0.0200, 0.0499, 0.9986]	[0.0199, 0.0498, 0.9986]	0.0081°
Group 2	[−0.0500, 0.0500, 0.9975]	[−0.0499, 0.0499, 0.9975]	0.0080°
Group 3	[0.0500, −0.0500, 0.9975]	[0.0498, −0.0499, 0.9975]	0.0128°
Group 4	[0.1000, −0.1000, 0.9899]	[0.0999, −0.0998, 0.9900]	0.0135°
Group 5	[0.0000, 0.1000, 0.9950]	[−0.0001, 0.0998, 0.9950]	0.0126°

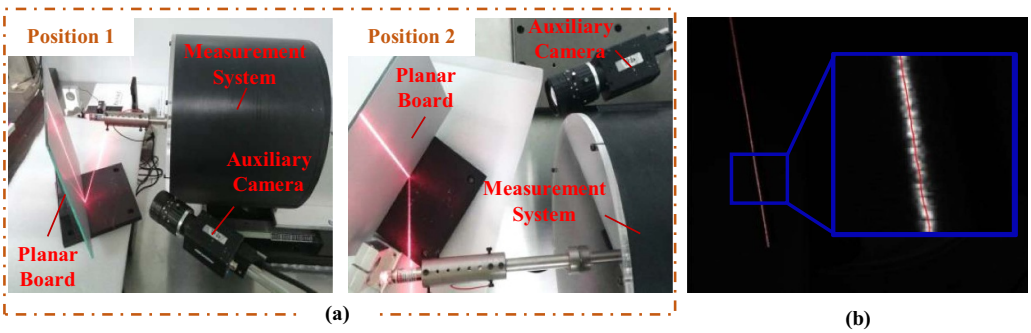

Figure 7. (a) Structured light calibration experiments in two position: auxiliary camera on left (Position 1) and auxiliary camera on right (Position 2); (b) one image of the line light stripe and the central point extraction result.

the system camera. The entire measurement system is mounted on a linear stage whose travel range is 300 mm with a stepper motor. Its minimum step interval is 1 μm. The captured images are transferred to the PC via a USB 3.0 cable and then processed in Matlab. A motion control card is used to control the stepper motor and read the motion position feedback.

4.2. Simulation experiment

Before the actual calibration experiment, the effect of the parameter optimization on the calibration described in section 3.1 needs to be verified by the simulation experiment. The circle-structured light measurement system model is established based on the design model of the real system. In the design model, the circle-structured light parameters are [0.0000, −0.0000, 1.0000, 300.0000], so the light plane parameters (A B C D) are set to [0.0499, −0.0499, 0.9975, 302.0000] by adding the deviation representing the assembly error to the model in the simulation.

The simulation experiment is divided into two groups. In the first group experiment, the system measures the inner radius of an 80 mm radius ring gauge placed at 10 different random positions with the same orientation. In the second group experiment, the system measures the same ring gauge placed at 10 different random positions with different random orientations. The coordinates of the intersecting points between the light plane and the inner surface are calculated, and the image pixel coordinates are calculated by the pinhole model of the system camera built according to the camera type and camera lens type in real system. Gaussian noise with 0.1 variance is added to the pixel coordinates to simulate the calculation error in extracting the central points of the ring light stripes.

Five initial structured light parameters to be respectively optimized using the simulation data of the two experimental groups are randomly preset to represent the results of the parameters obtained from the multi-position binocular-structured light calibration. The optimization results of two simulation experiment groups are shown in table 1. It can be seen that the optimization results of the second experiment group are obviously close to the true value, which proves the reliability of the optimization process. However, the results of the first experimental group are not close to the true value from different initial parameters because the minor axis length of the ellipse generated by the intersection of any structured light plane and the standard ring gauge is fixed. A comparison of the results

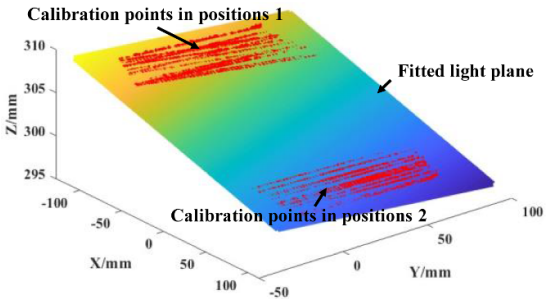

Figure 8. Parameters calibration result of circle-structured light plane.

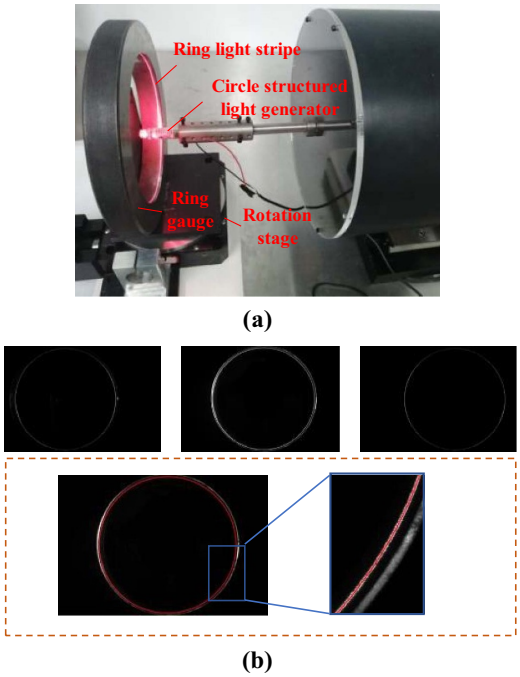

Figure 9. (a) The measurement of the ring gauge; (b) images captured in the experiment and the central point extraction result.

of the two experimental groupsindicates that the optimization cannot guarantee the uniqueness and correctness of the optimized light plane parameters if the ring gauge does not change its orientation during the calibration process. Therefore, the ring gauge must be measured in different orientations in real calibrations.

Next, the motion direction calibration process described in section 3.2 is verified by a simulation experiment. The motion direction of the stage is preset with the direction deviation from 0° to 15° representing the systematic error of the motion direction deviation of the linear stage. The simulation scanning measurement data of the inner surface of an 80 mm radius ring gauge in 0.1 mm step is calculated and Gaussian noise with 0.1 variance is added to the data. The motion direction of the stage is obtained through an optimization process using simulation data, and the correctness of the optimization algorithm is verified by comparing it with the preset and the optimized directions. Five simulation experiments are carried out, and different motion directions are preset in them. The main axis

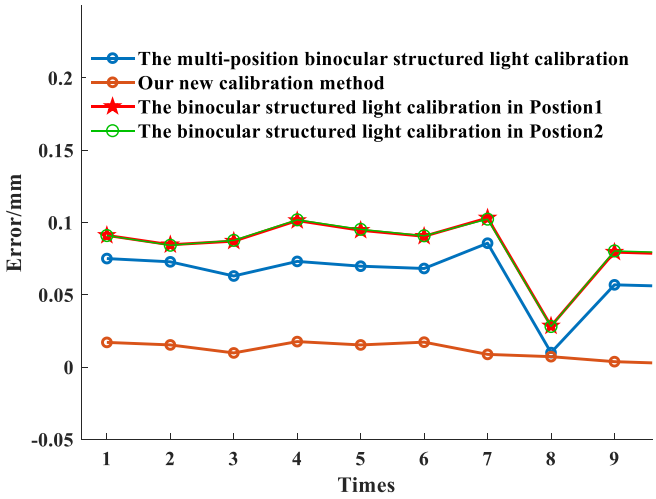

Figure 10. The measurement error of radius using different calibration methods.

direction of the measurement system $[0, 0, 1]^T$ is as the initial value in optimization, and the optimization results are shown in table 2. The deviation between the optimized motion direction and the preset direction is about 0.01°, which indicates that this calibration method can accurately acquire the actual motion direction.

4.3. Calibration experiment

After the simulation experiments, an actual experiment is carried out to verify the effectiveness of our two-step calibration method. As shown in figure 7(a), an auxiliary camera of the same type as the system camera is used in the first calibration step. The planar board is made by coating alumina on a normal glass board and its roughness is about 5 μm. According to the calibration process described in section 3.1, the multi-position binocular-structured light calibration is carried out on the left side (position 1) and the right side (position 2) of the system. The light stripe images taken during calibration and the central points of the light stripe extraction results are shown in figure 7(b). The coordinates of the calibration points in two positions are unified into the measurement coordinate system, and light plane parameters are fitted. The fitting results are shown in figure 8. The initial calibration result is [0.0342, 0.0210, 0.9992, 303.10], and the root-mean-square error of fitting is 0.0586 mm.

Then, the inner radius of the standard ring gauge with the reference radius 79.998 mm is measured by the system to optimize this initial result in the second calibration step, as shown in figure 9(a). It is mounted on a rotation stage that is used to change the position and orientation of the ring gauge. The system is used to measure the inner radius of the ring gauge placed in 10 random different positions and orientations, and the initial results are optimized to improve the calibration accuracy. Figure 9(b) shows some captured images in the experiment and the extracted central points of light stripes. The optimal calibration result is [0.0354, 0.0183, 0.9992, 303.09].

Table 3. The inner radius measurement results (unit: mm).

	Recover along the default direction	Radius masurement deviation	Recover along the calibrated direction	Radius measurement deviation
Group 1	80.0196	0.0221	79.9994	0.0019
Group 2	79.9096	−0.0879	79.9886	−0.0089
Group 3	79.9660	−0.0315	79.9891	−0.0084
Group 4	80.0089	0.0114	79.9968	−0.0007
Group 5	79.9135	−0.0840	79.9803	−0.0172

In order to verify the correctness of the result, we measured the inner radius of this ring gauge placed in another 10 random different positions with different orientations that ranged from −10° to 10°. The measurement results are respectively calculated using the structured light plane parameters obtained by the binocular-structured light calibration [19] in positions 1 and 2, respectively, by the multi-position binocular-structured light calibration and by our new calibration method. The errors of the measurement results are shown in figure 10. It can be seen that there are fewer measurement errors using parameters obtained by the multi-position binocular-structured light calibration than those using parameters obtained by the binocular-structured light calibration method, which validates that the multi-position binocular-structured light calibration can improve the calibration accuracy due to the larger observation range of the structured light plane. The mean error of the radius measurement results using parameters obtained by our calibration method is 11.5 μm with 6.8 μm standard deviation, and the average relative error is 0.015%. Compared with the results obtained by other methods, the measurement accuracy and repeatability have been improved by the new calibration method in our homemade system.

After the structured light calibration, the motion direction of the stage is calibrated in the second calibration step. In the experiment, the stage drives the system to measure the 10 mm inner surface in 0.5 mm step intervals of the same standard ring gauge, and its motion direction is acquired through the optimization process introduced in section 3.2. The calibration result is $\mathbf{M} = [0.0566, -0.0080, 0.9984]^T$. To verify the correctness of this result, the 10 mm inner surface of the ring gauge placed in five random different positions and orientations is measured in 0.5 mm step intervals. Five groups of measured data are respectively recovered along the main axis direction of the system and the calibrated motion direction M, and the inner radius measurement results are calculated by the cylinder fitting [30]. The results are shown in table 3, and demonstrate that the radius measurement results are more accurate using the calibrated motion direction to reconstruct the inner surface.

The measurement results of the third group are selected to register with the model of the ring gauge to analyze the measurement error distribution. The error distribution of the reconstructed surfaces along the default direction and the calibration direction is shown in figure 11. From the results, it can be seen that motion direction calibration can ensure surface reconstruction accuracy in scanning measurement and effectively compensate the systematic errors.

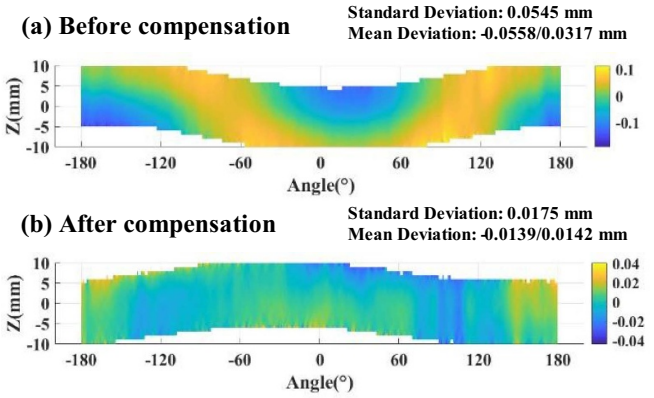

Figure 11. The error distribution of the recovered surface before and after compensation.

After calibration, the system is used to scanning measure the inner surface of the ring gauge fixed at a random position five times to verify the measurement repeatability. The error distribution of these five measurement results is shown in figure 12. It can be seen that the error distribution and measurement deviation are similar in the five results, proving the high measurement repeatability of the system.

4.4. Measurement application

In the calibration experiments, the results proved that the system can realize high-precision and high-repeatability measurements after using the proposed calibration method. For actual measurement applications in industry, the calibrated system is used to inspect the machining quality of a self-lubricating bearing sleeve sample without graphite columns installed on it. As shown in figure 13(a), the reference machining precision of this sleeve is 0.05 mm and its reference inner diameter is 155 mm and it has 28 × 12 mm diameter holes in it. In the measurement, the system is moved to capture 840 images during 84 mm in 0.1 mm step to measure the inner surface of this sleeve. The measurement result consists of 557 508 points, and the error distribution of the measurement result is shown in figure 13(b). The measurement result of the inner diameter is 155.019 mm and the diameter measurement results obtained by a cylinder fitting algorithm using the measured data near holes of the 28 holes on the sleeve have 7.9 μm mean error and 8.8 μm standard deviation, as is shown in figure 13(c). The experiment result further demonstrates that

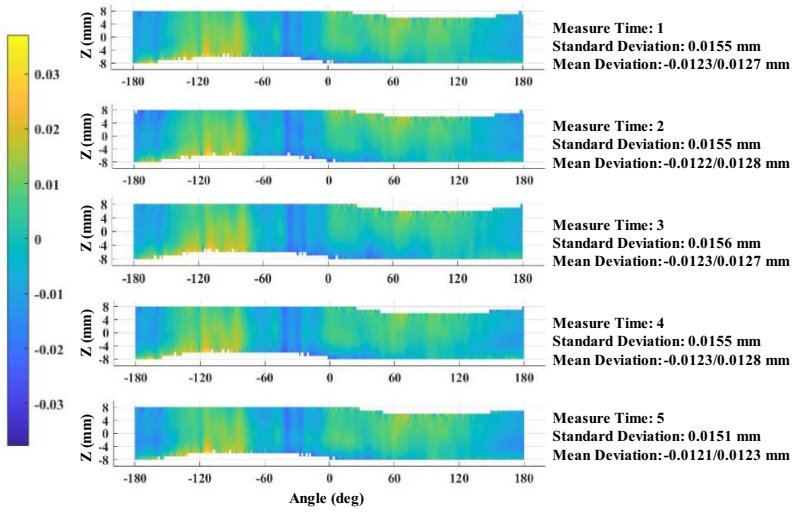

Figure 12. The error distribution of five measurement results of the ring gauge inner surface.

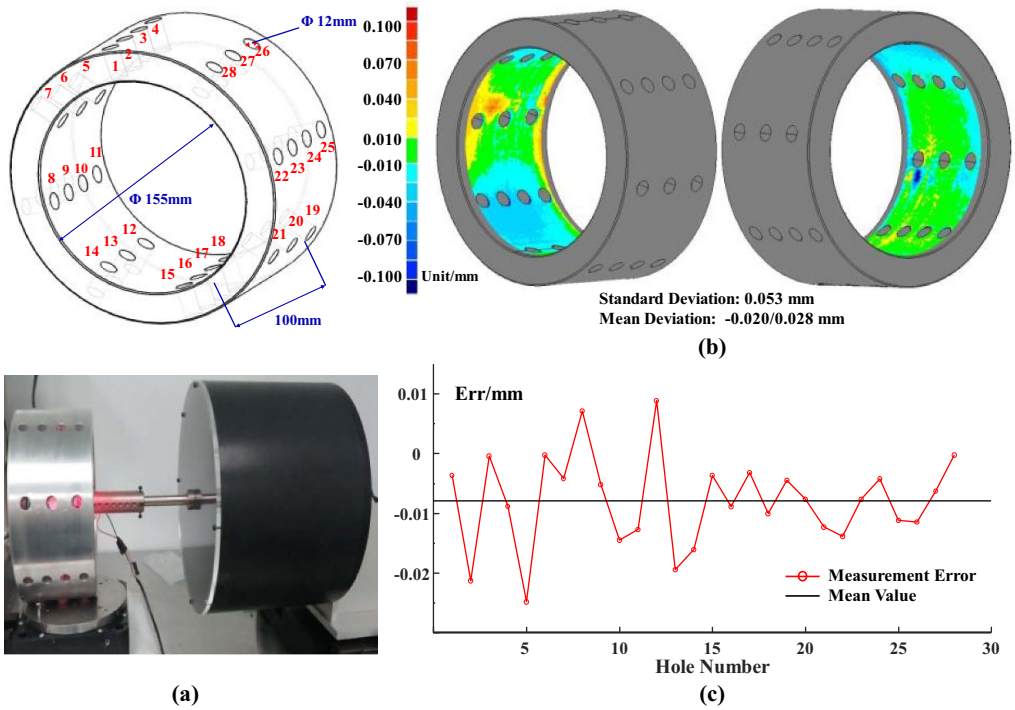

Figure 13. (a) The model of the measured self-lubricating bearing sleeve sample with hole number and the measurement of the ring gauge; (b) the error distribution of the measurement results of the sample; (c) the measurement error of hole diameter.

the circle-structured light measurement system calibrated by our proposed calibration method can satisfy high-precision measurement requirements in actual applications, such as in industrial fields.

5. Conclusion

This paper proposes a new two-step system calibration method for the circle-structured light inner surface measurement system to compensate the systematic errors of the light plane deviation and the motion direction deviation. In the first step, multi-position binocular-structured light calibration is conducted to obtain a more accurate initial calibration result based on a larger observation range of the light plane without interference by the system structure. Then, in the second step, it is optimized using the radius measurement results of a standard ring gauge placed in different random positions and orientations to improve the calibration accuracy. Using this optimized result, the motion direction is also calibrated by optimization using inner surface scanning measurement

data of a standard ring gauge to make a further improvement on the scanning measurement accuracy. In this method, the system calibration accuracy is improved by an optimization process using the standard ring gauge measurement data in the second step to reduce the influence of the binocular measurement error in the first calibration step. Meanwhile, the proposed method is easy to implement in actual applications to realize high-accuracy measurements without intricate calibration operations. In addition, this method only needs another camera, a blank planar board and a standard ring gauge. It does not require complex calibration targets or other expensive equipment. In our homemade system, the experimental results show that the mean relative measurement error can reach 0.015%, which validates that the system can realize high-precision and high-repeatability inner surface measurement via the proposed two-step calibration method in actual measurement applications. The new calibration method means that circle-structured light systems can potentially meet industrial measurement demands with high accuracy.

Acknowledgments

This research was funded by the National Key Research and Development Program of China (Grant No. 2017YFA 0701200); Science Challenge Program (Grant No. TZ2018 006-0203-01); Tianjin Natural Science Foundation of China (Grant No. 19JCZDJC39100).

ORCID iD

Xiaodong Zhang https://orcid.org/0000-0001-8469-7113

References

[1] Ji W, Jacobi A M, He Y and Tao W 2015 Summary and evaluation on single-phase heat transfer enhancement techniques of liquid laminar and turbulent pipe flow *Int. J. Heat Mass Transfer* **88** 735–54

[2] Silaipillayarputhur K, Al Mughanam T, Al Mojil A and Al Dhmoush M 2017 Analytical and numerical design analysis of concentric tube heat exchangers–a review *IOP Conf. Ser.: Mater. Sci. Eng.* **272** 012006

[3] Bilen K, Cetin M, Gul H and Balta T 2009 The investigation of groove geometry effect on heat transfer for internally grooved tubes *Appl. Therm. Eng.* **29** 753–61

[4] Hou W, Zhu J, Yang T and Jin G 2015 Construction method through forward and reverse ray tracing for a design of ultra-wide linear field-of-view off-axis freeform imaging systems *J. Opt.* **17** 055603

[5] Sansoni G, Bellandi P and Docchio F 2013 3d system for the measurement of tube eccentricity: an improved, rugged, easy to calibrate layout *Meas. Sci. Technol.* **24** 035901

[6] Gao H, Zhang X and Fang F 2017 Interferometry of a reflective axicon surface with a small cone angle using an optical inner surface *Meas. Sci. Technol.* **28** 095204

[7] Xu M, Kauth F, Mickan B and Brand U 2016 Traceable profile and roughness measurements inside small sonic nozzles with the profilscanner to analyse the influence of inner topography on the flow rate characters *Meas. Sci. Technol.* **27** 094001

[8] Liu Z and Krys D 2012 The use of laser range finder on a robotic platform for pipe inspection *Mech. Syst. Signal Process.* **31** 246–57

[9] Yokota M and Adachi T 2011 Digital holographic profilometry of the inner surface of a pipe using a current-induced wavelength change of a laser diode *Appl. Opt.* **50** 3937–46

[10] Yokota M, Koyama T and Takeda K 2017 Digital holographic inspection system for the inner surface of a straight pipe *Opt. Laser Eng.* **97** 62–70

[11] Viotti M R, Albertazzi A, Fantin A V and Dal Pont A 2008 Comparison between a white-light interferometer and a tactile formtester for the measurement of long inner cylindrical surfaces *Opt. Laser Eng.* **46** 396–403

[12] Inari T, Takashima K, Watanabe M and Fujimoto J 1994 Optical inspection system for the inner surface of a pipe using detection of circular images projected by a laser source *Measurement* **13** 99–106

[13] Wakayama T, Takahashi Y, Ono Y, Fujii Y, Gisuji T, Ogura T and Higashiguchi T 2018 Three-dimensional measurement of an inner surface profile using a supercontinuum beam *Appl. Opt.* **57** 5371–9

[14] Ritter M and Frey C W 2010 Rotating optical geometry sensor for inner pipe-surface reconstruction *Proc. SPIE* **7538** 753803

[15] Zhou F, Peng B, Cui Y, Wang Y and Tan H 2013 A novel laser vision sensor for omnidirectional 3D measurement *Opt. Laser Eng.* **45** 1–12

[16] Beermann R, Bossemeyer H, Diekmann R, Kästner M and Reithmeier E 2020 Model-based calibration routine for a triangulation sensor for inner radius measurements of cylindrical components *Proc. SPIE* **11352** 113520S

[17] Wang Y, Zhang R and Zhang Y 2012 Constructing method of calibration feature points used for circle structure light vision sensor *J. Appl. Opt.* **33** 884–8

[18] Zhu Y, Gu Y, Jin Y and Zhai C 2016 Flexible calibration method for an inner surface detector based on circle structured light *Appl. Opt.* **55** 1034–9

[19] Zhu Y, Wang L, Gu Y, Bi S, Zhai C, Jiang B and Ni J 2018 Three-dimensional inner surface inspection system based on circle-structured light *J. Manuf. Sci. Eng.* **140** 121007

[20] Zhang W and Zhuang B 1998 Non-contact laser inspection for the inner wall surface of a pipe *Meas. Sci. Technol.* **9** 1380–7

[21] Buschinelli P, Pinto T, Silva F, Santos J and Albertazzi A 2015 Laser triangulation profilometer for inner surface inspection of 100 millimeters (4″) nominal diameter *J. Phys.: Conf. Ser.* **648** 012010

[22] Buschinelli P D V, Melo J R C, Albertazzi Jr A, Santos J M and Camerini C S 2013 Optical profilometer using laser based conical triangulation for inspection of inner geometry of corroded pipes in cylindrical coordinates *Proc. SPIE* **8788** 87881H

[23] Zhang G and Wei Z 2002 A novel calibration approach to structured light 3D vision inspection *Opt. Laser Technol.* **34** 373–80

[24] Zhang G, He J and Li X 2005 3D vision inspection for internal surface based on circle structured light *Sensors Actuators* A **122** 68–75

[25] Fang C, Zhu L, Yan N and Zhang X 2020 Bilayer synchronous measuring method of curved screen based on a line-structured light-scanning sensor *Appl. Opt.* **59** 929–39

[26] Zhang Z 2000 A flexible new technique for camera calibration *IEEE Trans. Pattern Anal. Mach. Intell.* **22** 1330–4

[27] Jin L, Miyatsu N, Kondoh E, Gelloz B, Kanazawa N and Yoshizawa T 2018 Measurement of diameter of cylindrical openings using a disk beam probe *Opt. Rev.* **25** 656–62

[28] Moré J J 1978 The Levenberg-Marquardt algorithm: implementation and theory *Numerical Analysis* (Berlin: Springer) pp 105–16

[29] Fitzgibbon A, Pilu M and Fisher R B 1999 Direct least square fitting of ellipses *IEEE. Trans. Pattern. Anal.* **21** 476–80

[30] Lukács G, Martin R and Marshall D 1998 Faithful least-squares fitting of spheres, cylinders, cones and tori for reliable segmentation *European Conf. on Computer Vision* (Berlin: Springer) (https://doi.org/10.1007/BFb0055697)